PAPER

Vibrational excitation and dissociation of deuterium molecule by electron impact

IOP Publishing Plasma Physics and Controlled Fusion
Plasma Phys. Control. Fusion **63** (2021) 085006 (10pp) https://doi.org/10.1088/1361-6587/ac0163

Vibrational excitation and dissociation of deuterium molecule by electron impact

V Laporta[1,*], R Agnello[2], G Fubiani[3], I Furno[2], C Hill[4], D Reiter[5] and F Taccogna[1]

[1] Istituto per la Scienza e Tecnologia dei Plasmi, CNR, 70126 Bari, Italy
[2] Ecole Polytechnique Fédérale de Lausanne, Swiss Plasma Center, CH-1015 Lausanne, Switzerland
[3] LAPLACE, Université de Toulouse, CNRS, 31062 Toulouse, France
[4] Nuclear Data Section, International Atomic Energy Agency, Vienna A-1400, Austria
[5] Institute for Laser and Plasma Physics, Heinrich-Heine-University, D-40225 Düsseldorf, Germany

E-mail: vincenzo.laporta@istp.cnr.it

Received 10 February 2021, revised 13 May 2021
Accepted for publication 14 May 2021
Published 11 June 2021

Abstract

A theoretical investigation of electron-D_2 resonant collisions—via the low-lying and the Rydberg states of D_2^-—is presented for vibrational excitation, dissociative electron attachment and dissociative excitation processes by using the local-complex-potential approach. Full sets of vibrationally resolved cross sections, involving the ground electronic state—$X\,^1\Sigma_g^+$—and the first two electronic excited states—$b\,^3\Sigma_u^+$ and $B\,^1\Sigma_u^+$—of the D_2 molecule, are given for fusion plasma applications in their technologically relevant partially dissociated, detached divertor regimes. In particular, transitions between electronic excited states are also considered. Comparisons are made with cross sections present in the literature, where available.

Keywords: deuterium, electron collisions, plasma fusion, divertor, cross sections

(Some figures may appear in colour only in the online journal)

1. Introduction

Electron-impact vibrational excitation (VE) and dissociation of deuterium molecules are of primary importance in many fields, ranging from astrophysics and plasma discharges to nuclear fusion, including fundamental physics [1].

Molecular hydrogen H_2, deuterated hydrogen HD and deuterium D_2, the simplest and at the same time the most abundant species formed in the pregalactic gas prior to structure formation, played an important role in the cooling of the gas clouds which gave birth to the first stellar generation [2, 3]. In this regard, it has been shown that the D/H ratio in giant planets, Jupiter and Saturn, is a fundamental parameter to understand the formation of the Solar System from the primitive nebula [4]. Moreover, electron-impact cross sections for HD, D_2 and the corresponding ions are needed to explain certain phenomena occurring in the different planetary atmospheres and their ionospheres [5].

Among technological applications, electron-D_2 collision cross sections are strictly related to the important problem of plasma interaction with the neutral gas component originating from surface recombination, from volumetric recombination channels, and/or from external gas puffing (plasma fueling). This is of particular relevance for the so-called 'detached divertor regime' in magnetic fusion devices [6, 7], which is currently intensively studied in existing tokamaks and stellarators, and is also foreseen as the standard operational mode for the ITER fusion reactor under construction in Cadarache (South France). In this detached plasma mode of operation the hydrogenic plasma chemistry plays a key role for critical issues such as plasma energy and momentum dissipation, high heat flux component protection and particle (ash) removal. There molecular reaction kinetics comprises an important

* Author to whom any correspondence should be addressed.

sub-model of the integrated multi-physics boundary plasma code systems, such as e.g. SOLPS-ITER, which was and still is heavily used for guiding the ITER divertor design [8], and future experimental campaigns.

Powerful volumetric plasma-gas interaction mechanisms are known to be operative in fusion machine reactors, involving both resonant electron collisions—via resonant D_2^- anion states—and near resonant positive atomic ion (ion conversion, such as charge transfer channels) reactions. Such resonant processes are believed to be a key ingredient towards a quantitative understanding of the near target divertor plasma dynamics, with their prominent effects also on dissociation degree, perhaps molecular-assisted additional volumetric recombination channels, but certainly for establishing the vibrational distribution of electronic ground molecules. Eliminating this latter from the unknown parts of fusion divertor models by a reliable cross section database can be expected to greatly improve the predictive and interpretative quality in current fusion reactor divertor models and spectroscopy interpretation tools. A recent account of the status of including such resonant channels in fusion relevant collision radiative models is given in [9], in which data for these resonant channels are deduced from [10].

Another very important application in nuclear fusion field is related to negative ion sources for neutral beam injection system. In particular, electron-D_2 vibrationally resolved processes are of paramount importance for kinetic models [11] simulating the production, transport, extraction, acceleration and neutralization of negative ion beams to heat thermonuclear reactors. In this regard, a relevant result is that sources operated with deuterium could not achieve the same performances as a source operated with hydrogen at the same power and pressure [12], indicating a strong isotopic dependence from nuclear motion effects in these resonance channels, quite distinct from non-resonant electron collision systems. A recent detailed experimental study of this well established isotope effect in dissociative attachment (DA) resonance channels is given by Krishnakumar *et al* [13].

A complete and updated set of deuterium cross sections is crucial to model the plasma of negative ion sources for fusion, which are currently routinely operated both with hydrogen and deuterium [14]. Since the availability and access of plasma diagnostics in these devices is limited due to construction and operation constraints imposed by source optimization, it is difficult to precisely monitor plasma parameters in the entire source volume. A small size, low pressure helicon plasma such as RAID [15], able to achieve high power hydrogen and deuterium discharges and mimic the electron temperature and density conditions of both the driver and the expansion region of large negative ion sources for fusion, represents a versatile testbench to validate numerical models. Dedicated particle-in-cell and fluid modeling are currently underway to shed light on transport and chemistry of hydrogen RAID plasma discharges [16].

Aimed at supplying data for non-equilibrium plasma modeling applications [17–19], a large number of theoretical [20–23] and experimental [24–27] works, including a review [28], have appeared for H_2 cross sections. Moreover, recently, results for H_2^+ collisions with electrons [29–31], for the process of dissociative recombination, have become available. In spite of that, very little information exists in the literature about D_2 excitation and dissociation and, more generally, for the nuclear fusion relevant D_2, DT and T_2 collision systems proceeding via their anion resonances.

In order to fill the lack of data, in this paper, we will consider vibrationally-resolved resonant collisions by electron-impact, for the processes of VE, DA and dissociative excitation (DE), reported in table 1, involving the ground electronic state—$X\,^1\Sigma_g^+$—and the first two electronic excited states—$b\,^3\Sigma_u^+$ and $B\,^1\Sigma_u^+$—of the D_2 molecule, which proceed through the low lying and the Rydberg states of D_2^- resonances.

With regard to resonant scattering, it has been largely demonstrated that, for the collisions with electrons at low energy, it gives the dominant contribution in plasma kinetics [32–34]. The cross section calculations will be performed in the so-called 'local-complex-potential' (LCP) approach [35–38] and for the first time this methodology will be applied for vibrational transitions among excited electronic states.

In this work, we are interested in resonant scatterings: the adiabatic nuclei approximation, often used to study electron molecule collision systems (see e.g. the molecular convergent close-coupling calculations in [21] and references therein), cannot be applied in this context. While the Rydberg resonances—via high lying Rydberg states of the D_2^- anion—have received attention in recent literature, the hitherto poorly studied low lying resonances (via the $X\,^2\Sigma_u^+$ state of D_2^-), are of particular relevance for the 0.5–5 eV electron temperatures in typical fusion detached divertor plasma scenarios. It is particularly this gap which we aim at in this paper with up to date and *ab initio* theoretical calculations.

The manuscript is organized as follows: in section 2 we give a brief overview on the Local Complex Potential theoretical model used in the calculations and on the molecular input data; in section 3 we discuss the results within a comparison with cross sections presented in literature where available and we show the isotopologue effect with H_2. Finally, conclusions are present in section 4 of the paper.

2. Theoretical model

In this section, we briefly introduce the LCP model: the theoretical framework we used to describe the resonant scattering processes presented in table 1. In the phenomenology of resonant collisions, as a first step, the incident electron is temporarily captured by the neutral target molecule forming a unstable anionic system, the resonance, which is represented by the intermediate state in the reactions in the table 1. After a characteristic lifetime—related to the so-called 'resonance width'—the negative compound decays, leading to a large spectrum of different final states, competing with each other, including excitation or dissociation of the initial molecule.

The LCP model is an effective quantum *ab initio* approach which takes into account the molecular nuclear dynamics and

Table 1. List of the elementary processes, vibrationally-resolved, considered in the text. v and v' represent the vibrational levels and ϵ_c the energy of continuum of the electronic states of D_2 molecule.

Label	Reaction
	Vibrational excitation
VE1	$e(\epsilon)+D_2(X^1\Sigma_g^+;v)\rightarrow D_2^-(X^2\Sigma_u^+,B^2\Sigma_g^+,C^2\Sigma_g^+)\rightarrow e(\epsilon')+D_2(X^1\Sigma_g^+;v')$
VE2	$e(\epsilon)+D_2(X^1\Sigma_g^+;v)\rightarrow D_2^-(C^2\Sigma_g^+)\rightarrow e(\epsilon')+D_2(B^1\Sigma_u^+;v')$
VE3	$e(\epsilon)+D_2(B^1\Sigma_u^+;v)\rightarrow D_2^-(C^2\Sigma_g^+)\rightarrow e(\epsilon')+D_2(B^1\Sigma_u^+;v')$
	Dissociative electron attachment
DA1	$e(\epsilon)+D_2(X^1\Sigma_g^+;v)\rightarrow D_2^-(X^2\Sigma_u^+,B^2\Sigma_g^+)\rightarrow D(1s)+D^-(1s^2)$
DA2	$e(\epsilon)+D_2(X^1\Sigma_g^+;v)\rightarrow D_2^-(C^2\Sigma_g^+)\rightarrow D(n=2)+D^-(1s^2)$
DA3	$e(\epsilon)+D_2(B^1\Sigma_u^+;v)\rightarrow D_2^-(C^2\Sigma_g^+)\rightarrow D(n=2)+D^-(1s^2)$
	Dissociative excitation
DE1	$e(\epsilon)+D_2(X^1\Sigma_g^+;v)\rightarrow D_2^-(X^2\Sigma_u^+,B^2\Sigma_g^+,C^2\Sigma_g^+)\rightarrow e(\epsilon')+D_2(X^1\Sigma_g^+;\epsilon_c)\rightarrow e(\epsilon')+D(1s)+D(1s)$
DE2	$e(\epsilon)+D_2(X^1\Sigma_g^+;v)\rightarrow D_2^-(B^2\Sigma_g^+,C^2\Sigma_g^+)\rightarrow e(\epsilon')+D_2(b^3\Sigma_u^+;\epsilon_c)\rightarrow e(\epsilon')+D(1s)+D(1s)$
DE3	$e(\epsilon)+D_2(X^1\Sigma_g^+;v)\rightarrow D_2^-(C^2\Sigma_g^+)\rightarrow e(\epsilon')+D_2(B^1\Sigma_u^+;\epsilon_c)\rightarrow e(\epsilon')+D(2p)+D(1s)$
DE4	$e(\epsilon)+D_2(B^1\Sigma_u^+;v)\rightarrow D_2^-(C^2\Sigma_g^+)\rightarrow e(\epsilon')+D_2(B^1\Sigma_u^+;\epsilon_c)\rightarrow e(\epsilon')+D(2p)+D(1s)$
DE5	$e(\epsilon)+D_2(B^1\Sigma_u^+;v)\rightarrow D_2^-(C^2\Sigma_g^+)\rightarrow e(\epsilon')+D_2(b^3\Sigma_u^+;\epsilon_c)\rightarrow e(\epsilon')+D(1s)+D(1s)$
DE6	$e(\epsilon)+D_2(B^1\Sigma_u^+;v)\rightarrow D_2^-(C^2\Sigma_g^+)\rightarrow e(\epsilon')+D_2(X^1\Sigma_g^+;\epsilon_c)\rightarrow e(\epsilon')+D(1s)+D(1s)$

Table 2. Dissociating channels converging to the electronic states of D_2 and D_2^- considered in the text. Asymptotic limit positions are given with respect to the $D(1s)+D(1s)$ threshold.

Channel	Limit	Energy (eV)	Symmetries
DE3, DE4	$D(2p)+D(1s)$	+10.17	$B^1\Sigma_u^+$
DA2, DA3	$D(n=2)+D^-(1s^2)$	+9.44	$C^2\Sigma_g^+$
DE1, DE2, DE5, DE6	$D(1s)+D(1s)$	0.00	$X^1\Sigma_g^+$, $b^3\Sigma_u^+$
DA1	$D(1s)+D^-(1s^2)$	–0.75	$X^2\Sigma_u^+$, $B^2\Sigma_g^+$

thus it is able to consider vibrational state resolved cross sections. We restrict ourselves to the major equations of LCP and for a comprehensive theoretical treatment of the resonant collisions by electron-impact, we refer back to the original papers [35–38] and references therein. Recently, the LCP model was widely used to determine low-energy dissociations by electron impact and VEs for the ground state of the molecules of NO [39, 40], CO [41] and molecular oxygen [42–44], which gave results in good agreement with experiment.

With respect to the reactions in the table 1, in the following, we will refer to the electronic states of D_2, by $\mathcal{S}=\{X^1\Sigma_g^+,b^3\Sigma_u^+,B^1\Sigma_u^+\}=\{X,b,B\}$ and to the D_2^- resonances, by $\mathcal{R}=\{X^2\Sigma_u^+,B^2\Sigma_g^+,C^2\Sigma_g^+\}=\{X^-,B^-,C^-\}$. The correspondence between symmetry states and reaction channels is reported in table 2.

According to the LCP approach, the cross sections for the VE, DA and DE processes—in the rest frame of a D_2 molecule initially in vibrational level v of the electronic state s and for an incident electron of energy ϵ—are given by:

$$\sigma^{\rm VE}_{s,v\rightarrow s',v'}(\epsilon)=\sum_{r\in\mathcal{R}}\frac{2S_r+1}{(2S_s+1)\,2}\frac{g_r}{g_s\,2}\frac{64\,\pi^5\,m^2}{\hbar^4}\frac{k'}{k}\times\left|\langle\chi^{s'}_{v'}|\mathcal{V}^{s'}_r|\xi^r_{s,v}\rangle\right|^2,\qquad s,s'\in\mathcal{S},\quad(1)$$

$$\sigma^{\rm DA}_{s,v}(\epsilon)=\sum_{r\in\mathcal{R}}\frac{2S_r+1}{(2S_s+1)\,2}\frac{g_r}{g_s\,2}2\pi^2\,\frac{K}{\mu}\,\frac{m}{k}\lim_{R\rightarrow\infty}\times\left|\xi^r_{s,v}(R)\right|^2,\qquad s\in\mathcal{S},\quad(2)$$

$$\sigma^{\rm DE}_{s,v}(\epsilon)=\sum_{r\in\mathcal{R}}\frac{2S_r+1}{(2S_s+1)\,2}\frac{g_r}{g_s\,2}\frac{64\,\pi^5\,m^2}{\hbar^4}\times\int_{\epsilon^{th}}^{\epsilon^{max}}d\epsilon_c\frac{k'}{k}\left|\langle\chi^{s'}_c|\mathcal{V}^{s'}_r|\xi^r_{s,v}\rangle\right|^2,\qquad s,s'\in\mathcal{S},\quad(3)$$

where $2S_r+1$ and $2S_s+1$ account for the spin-multiplicities of the resonant anion state and of the neutral target state, respectively, g_r and g_s represent the corresponding degeneracy factors, m is the electron mass, μ is the reduced mass of D_2 nuclei, and k represents the incoming electron momentum. For the VE and DE processes k' is the outgoing electron momentum whereas for the DA process K is the asymptotic momentum of the final dissociating fragments $D+D^-$. $\chi^{s'}_{v'}$ in equation (1) and $\chi^{s'}_c$ in equation (3) refer to the vibrational and continuum final wave function belonging to the electronic state s' of D_2, respectively. $\langle\cdot|\cdot|\cdot\rangle$ stands for integration over the internuclear coordinate R and the integral in the DE cross section extends into the continuum part of the D_2 potential from the dissociation threshold energy ϵ^{th}, corresponding to the initial vibrational level v, up to $\epsilon^{max}=\epsilon^{th}+50$ eV.

Table 3. Some spectroscopic proprieties and energy of vibrational levels for the $X\,^1\Sigma_g^+$ and $B\,^1\Sigma_u^+$ electronic states of D_2 molecule.

$D_2(X\,^1\Sigma_g^+)$		$D_2(B\,^1\Sigma_u^+)$			
$\mu = 1835.741$ a.u.					
$R_{eq} = 1.401$ a.u.		$R_{eq} = 2.417$ a.u.			
$D_e = 4.747$ eV		$D_e = 3.568$ eV			
$D_0 = 4.555$ eV		$D_0 = 3.508$ eV			
v	ϵ_v^X (eV)	v	ϵ_v^B (eV)	v	ϵ_v^B (eV)
0	0.000	0	11.222	25	13.536
1	0.371	1	11.339	26	13.605
2	0.727	2	11.454	27	13.673
3	1.069	3	11.566	28	13.738
4	1.397	4	11.677	29	13.802
5	1.710	5	11.785	30	13.865
6	2.010	6	11.891	31	13.926
7	2.295	7	11.994	32	13.986
8	2.566	8	12.096	33	14.043
9	2.823	9	12.196	34	14.099
10	3.066	10	12.294	35	14.154
11	3.294	11	12.390	36	14.207
12	3.506	12	12.484	37	14.258
13	3.703	13	12.575	38	14.308
14	3.883	14	12.666	39	14.357
15	4.045	15	12.754	40	14.403
16	4.189	16	12.840	41	14.448
17	4.312	17	12.924	42	14.491
18	4.414	18	13.007	43	14.532
19	4.490	19	13.088	44	14.571
20	4.538	20	13.167	45	14.606
		21	13.244	46	14.640
		22	13.320	47	14.670
		23	13.393	48	14.696
		24	13.466	49	14.718

In equations (1)–(3), $\xi^r_{s,v}(R)$ is the resonant wave function solution of the nuclear equation with total energy $E = \epsilon^s_v + \epsilon$:

$$\left[-\frac{\hbar^2}{2\mu}\frac{d^2}{dR^2} + V_r^-(R) - \frac{i}{2}\Gamma_r(R) - E\right]\xi^r_{s,v}(R) = -\mathcal{V}^s_r(R)\,\chi^s_v(R)\,, \qquad r \in \mathcal{R}, \tag{4}$$

where $V_r^-(R)$ and $\Gamma_r(R)$ represent the potential energies and the autoionization widths for the D_2^- resonant states included in the calculations and χ^s_v is the wave function for the initial vibrational state of electronic state s of D_2 with energy ϵ^s_v.

In the LCP formalism, $\mathcal{V}^s_r$ is the discrete-to-continuum coupling between the resonance r and the electronic state s of target given by:

$$\mathcal{V}^{s2}_r = \frac{\hbar}{2\pi}\frac{\Gamma^s_r}{k}, \qquad r \in \mathcal{R}, \tag{5}$$

where Γ^s_r is the partial width of the resonance r with respect to the electronic state s of the D_2 molecule. The relationship with the total width present in the equation (4) is given by:

$$\Gamma_r = \sum_{s\in\mathcal{S}}\Gamma^s_r, \qquad r \in \mathcal{R}. \tag{6}$$

In the calculations, we used the potential energy curves of the H_2 molecule for the ground state $X\,^1\Sigma_g^+$ [45, 46], for the first repulsive excited state $b\,^3\Sigma_u^+$ [47] and for the $B\,^1\Sigma_u^+$ [48] excited state but with a reduced mass $\mu = 1835.741$ a.u. of D_2 nuclei. For the resonant states D_2^-, the complex potential for the lowest valence was taken from papers [49, 50] whereas the data for the Rydberg excited state $C\,^2\Sigma_g^+$ come from the R-matrix calculation contained in the paper [51].

Figure 1 summarizes the molecular data—the potentials for D_2 and D_2^- as well as the partial widths for the three resonant states—used in the calculations. In the theoretical model, integration over internuclear distances carrier out over the interval $R \in [0.4, 15]$ a.u. The vibrational levels and the dissociation energies for the $X\,^1\Sigma_g^+$ and $B\,^1\Sigma_u^+$ states of D_2 molecule are reported in table 3. Potentials in figure 1 and vibrational levels in table 3 refer to rotational ground states ($j = 0$) in the present work, and all cross sections in the following correspond to rotational temperature $T_R = 0$, i.e. $j = j' = 0$ for all transitions.

3. Results and discussion

Figures 2 and 3 summarize the results of this work. They present an overview over the full set of cross sections vibrationally resolved for the ground electronic state $X\,^1\Sigma_g^+$ and for the excited electronic $B\,^1\Sigma_u^+$ state of the D_2 molecule obtained in the LCP approach, for the processes listed in the table 1. It should be noted, concerning the vibrational transitions, that only inelastic excitations, i.e. for $v' > v$, the so-called VEs, are shown in the plots: super-elastic transitions, also known as vibrational de-excitation (VdE) processes, i.e. for $v' < v$, can be obtained from the VE by the detailed balance principle. If $\sigma^{\rm VE}_{s,v\to s',v'}(\epsilon)$ represents the cross sections for the inelastic transition, the corresponding VdE process with electron energy ϵ' is given by:

$$\sigma^{\rm VdE}_{s',v'\to s,v}(\epsilon') = \sigma^{\rm VE}_{s,v\to s',v'}(\epsilon' + \epsilon^{th}_{s,v\to s',v'})\,\frac{\epsilon' + \epsilon^{th}_{s,v\to s',v'}}{\epsilon'}\,, \tag{7}$$

where $\epsilon^{th}_{s,v\to s',v'} = \epsilon^{s'}_{v'} - \epsilon^s_v$ is the threshold for the VE process considered.

Analogously, the associative detachment cross section, $\sigma^{\rm AD}_{s,v}$, and its inverse process of DA are linked by balance detail principle:

$$\sigma^{\rm AD}_{s,v}(E) = \sigma^{\rm DA}_{s,v}(E - \epsilon^s_v)\,\frac{m\,(E - \epsilon^s_v)}{\mu E}\,. \tag{8}$$

Many features can be observed in the cross sections for the ground state presented in figure 2. For low vibrational levels, $v < 5$, the magnitudes of DA processes, DE1 and DE3 are negligible compared with mono- and bi-quantic VE transitions. The dominant dissociating channel is represented by the DE2 process, through the $b\,^3\Sigma_u^+$ state, because of the strong couplings $B^- \to b$ and $C^- \to b$ (see plots on the right in

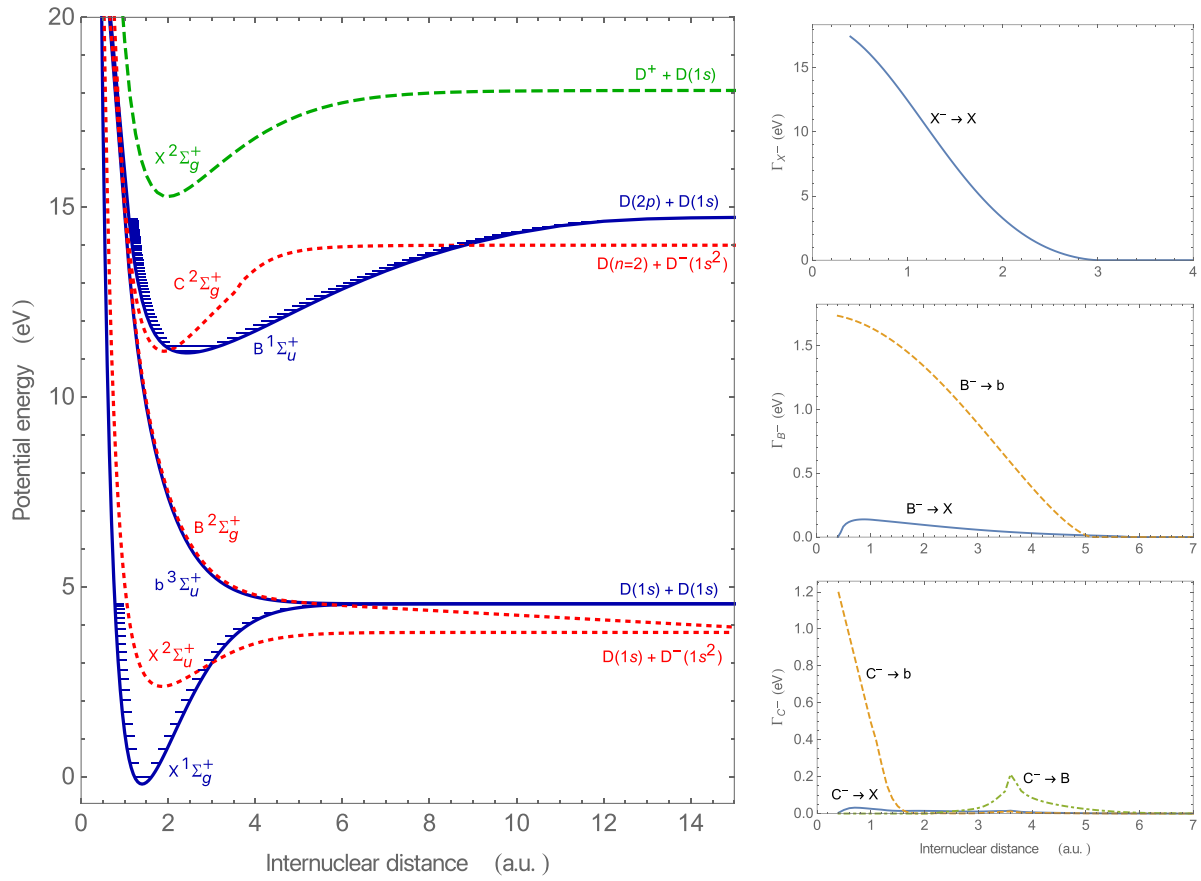

Figure 1. (Plot on the left) Potential energy curves of D_2 electronic states (solid blue lines) and of D_2^- resonances (dotted red lines) considered in the calculations. For sake of comparison the ground state of D_2^+ (broken green line) is also shown. (Plots on the right) Partial widths with respect to the neutral states of the three resonances included in the calculations as a function of the internuclear distance.

figure 1). As the vibrational levels increase and the first D_2^- threshold is reached, all DA and DE channels become important: for $5 < v < 12$ they are comparable to the VE and for high vibrational levels, for $v > 12$, they are the dominant processes. In particular, the DA1 channel become threshold-less processes and the dissociation from DE1 process has the same order of magnitude as DE2 channel.

Concerning specifically the VE cross sections, many oscillating structures can be observed in the figure 2. In particular, two sets of peaks can be distinguished: the first one ends at the DA1 threshold and the second one, at higher energies, corresponds to the DA2 process. This behavior can be traced back to the vibrational structures of the resonances in D_2^-. On the other hand, the processes VE2, i.e. the excitation to the $B\,^1\Sigma_u^+$ state from the ground state, due to the Frank-Condon factors, are inefficient for all vibrational levels and the corresponding cross sections are represented by narrow spikes around 11 eV.

Regarding the processes starting from the $B\,^1\Sigma_u^+$ state of D_2, figure 3, a remarkable feature is given by the dissociation toward the $b\,^3\Sigma_u^+$ state—channel DE5—which is the overall dominant process: this behavior is favored by kinetics and in particular by the strong coupling $C^- \to b$. On the opposite site, DE6 dissociation, which leads to the same threshold as DE5, is suppressed because of small coupling $C^- \to X$.

For high vibrational levels, as the threshold of the $C\,^2\Sigma_g^+$ resonance is reached, the DA process DE3 becomes important. As a matter of the fact no direct couplings exist between the $B\,^1\Sigma_u^+$ and the lower resonances (see plots in figure 1), DA toward the limit $D(1s) + D^-(1s^2)$ is forbidden.

To further illustrate the results of this work, figure 4 contains some selected reaction rates (Maxwellian electron distribution), for the ground state $X\,^1\Sigma_g^+$ of D_2 molecule and for the processes reported in table 1. These rates are given here for initial vibrational states $v = 0, 1, 10$ and 20, and plotted as a function of the electron temperature.

Globally, the behavior of the reaction rates follows those of the corresponding cross sections. For low vibrational levels, (see e.g. $v = 0, 1$), at low electron temperatures ($\lesssim 10^4$ K), multi-quantum VEs and de-excitations (broken curves) will play a important role in the plasma bulk whereas, at high temperatures ($>10^4$ K), dissociation (DE1+DE2, curves with circles in the figure) dominates and only mono- or bi-quantic transitions will contribute to the kinetics.

Regarding medium vibrational levels, (see e.g. $v = 10$), dissociative electron attachment process (DA1+DA2, curves with diamonds in the figure) overcomes the dissociation and for all range of electron temperatures is the major channel to dissociate the D_2 molecule. Vibrational transitions are important only at very low electron temperatures.

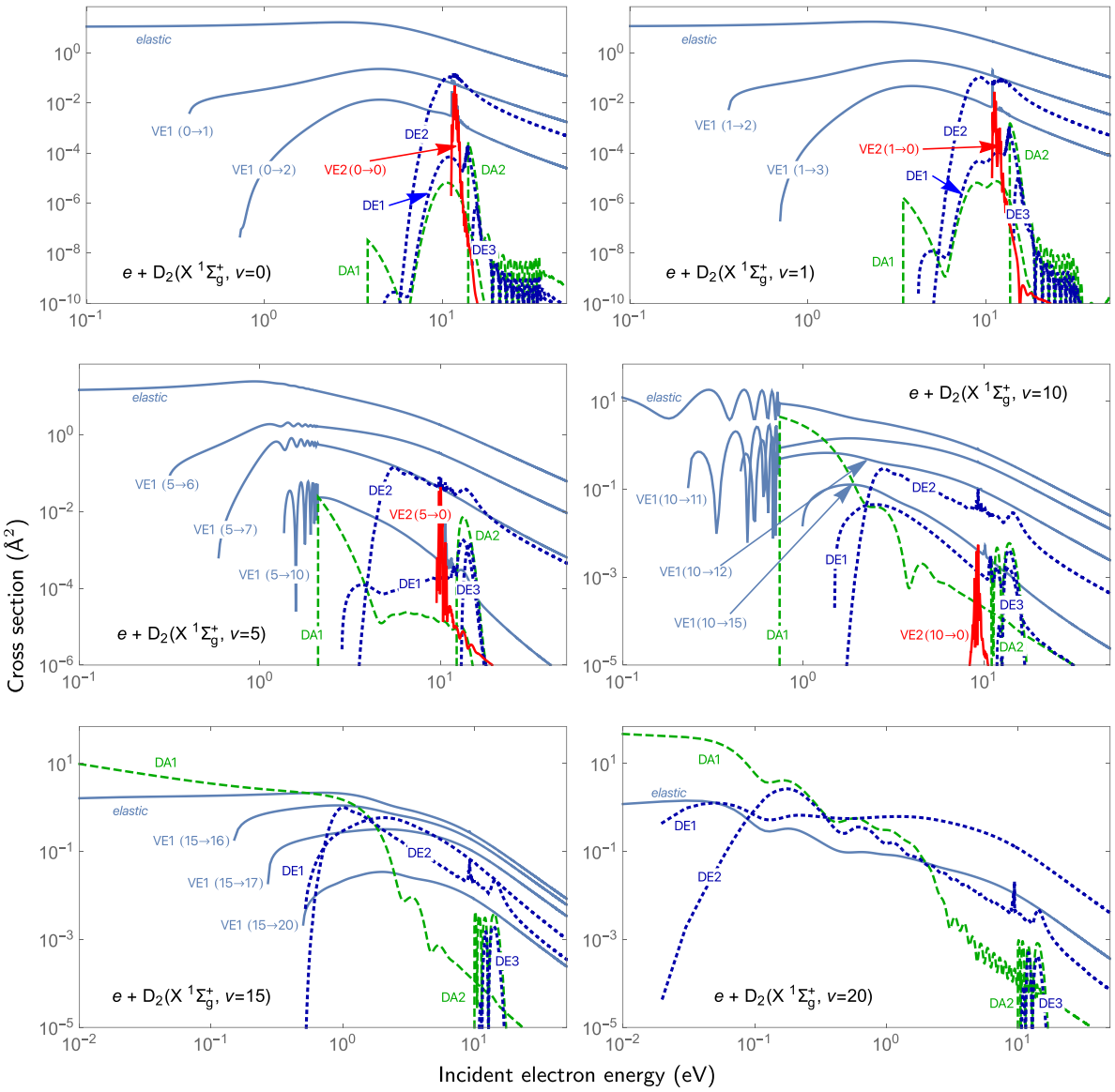

Figure 2. Overview of vibrationally resolved resonant cross sections by electron impact for the ground state $X\,^1\Sigma_g^+$ of D_2 molecule for the processes of vibrational excitation (elastic and VE, solid lines), dissociative attachment (DA, dashed lines) and dissociative excitation (DE, dotted lines) as obtained from the LCP model.

Finally, for very high vibrational levels, as expected, dissociation reactions, DA1+DA2 and DE1+DE2, dominate overall.

3.1. Comparison with data in the literature

In order to validate our LCP cross sections presented in section 3, in figure 5 we report comparisons with data available in the literature. In the first plot, good agreement we observed for the elastic process compared with the experimental results of Golden *et al* [52], in particular we correctly reproduce the main peak in the cross sections which has clearly a resonant nature. As expected, LCP calculations underestimate the behavior at high energy where non-resonant contributions become important. On the other hand, at very low energy, because nuclear spin effects are not included in our model, the LCP cross section is not able to reproduce the anomalous quasi-elastic electron scattering [53].

VE cross sections—i.e. the plots VE1($0 \to 1$), VE1($0 \to 2$) and VE1($0 \to 3$)—compare well with the experiments of Buckman and Phelps [54] and they present a similar global shape as Biagi's calculations [55] except for the peaks around 12 eV due to the $C\,^2\Sigma_g^+$ resonance. In the case of Biagi's theoretical results, unfortunately no details regarding the LXCat database nor on the theoretical method are given. The most widely used cross sections so far seem to be the ones given in [49], with numerical values at 6 eV and 8 eV collision energies.

Concerning the DA processes, in the plot 'D^- production', we reproduce correctly the experimental results of Schulz and Asundi [56] at low energies by DA1 cross section. At higher energies, our results are in agreement with experiments

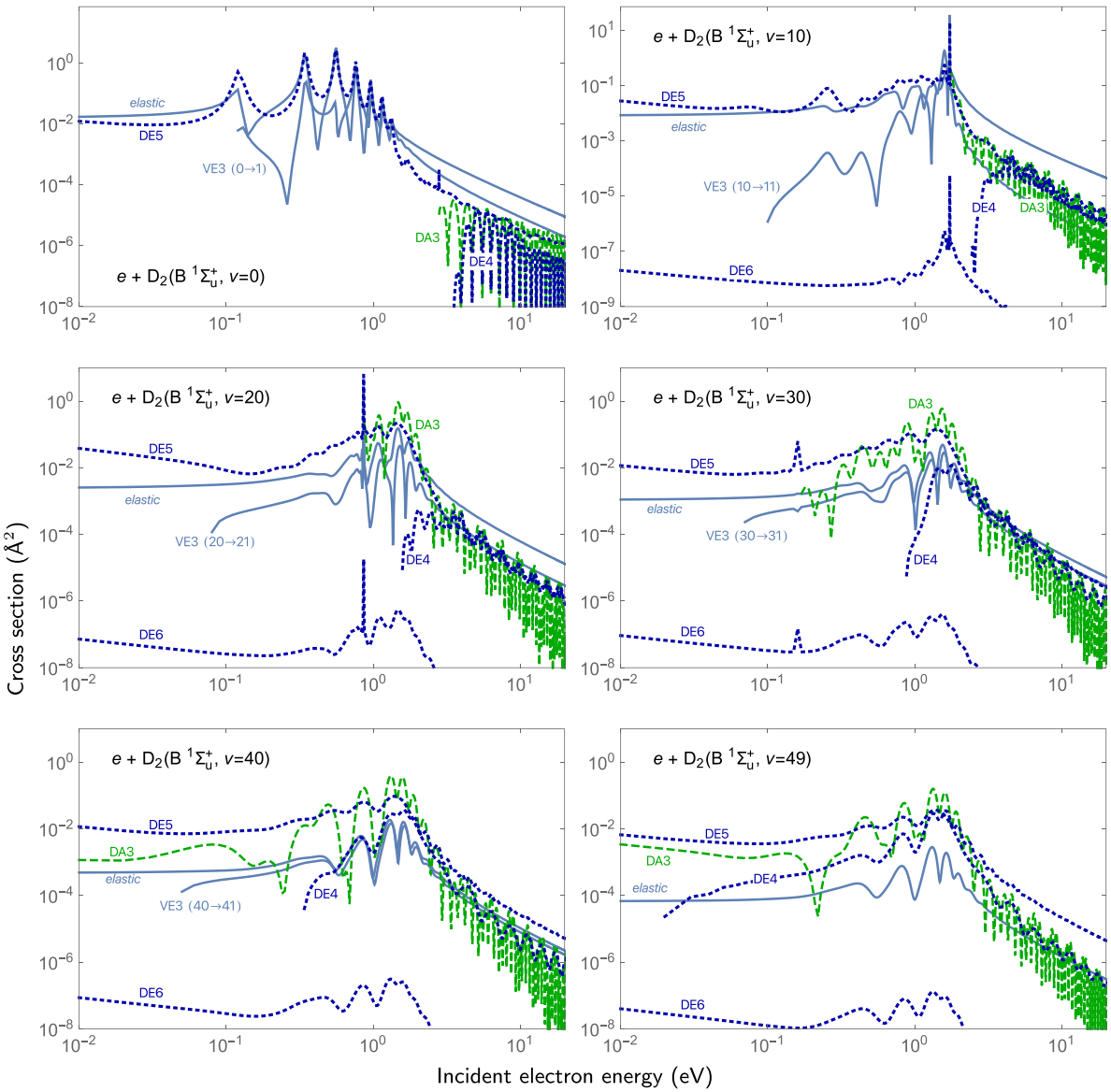

Figure 3. Same as in figure 2 but for the $B\,^1\Sigma_u^+$ excited state of D_2 molecule.

of Rapp *et al* [57], to which we removed the background from the cross section, and with the results of Krishnakumar *et al* [13]. In particular we reproduce correctly the structure around 10 eV from DA1 channel and the peak at 14 eV of DA2 process.

The last plot 'D+D production' compares our DE1 and DE2 channels for D2 dissociation with the results of Scarlett *et al* [58], Trevisan and Tennyson [59] and Yoon *et al* [60]. Cross sections in the papers [58–60] share the same theoretical approach of 'adiabatic nuclei' approximation—which is, in principle, able to include non-resonant contributions—and they refer to the dissociation only by the $b\,^3\Sigma_u^+$ state which corresponds to our DE2 channel. As expected, our resonant DE2 cross section reproduces correctly, at low energies, the total dissociation via the $b\,^3\Sigma_u^+$ state and falls short of it at high energies where non-resonant scattering dominates.

In the comparisons with experimental data, we checked the discrepancy with the present results is around 15%. We therefore assume for the presented cross sections an uncertainty of the same order of magnitude.

3.2. *Isotopologue effect*

Plots in figure 6 report the isotopologue effect of D_2 and H_2 molecules on cross sections for some selected processes. We have calculated, in the same LCP theoretical approach as for D_2, some of the corresponding cross sections also for the H_2 system. A full comparative study with all cross sections will be subject to future work.

The first difference we remark is in the threshold: in fact, because the vibrational levels for H_2 are systematically shifted up compared to those of D_2 with same vibrational quantum

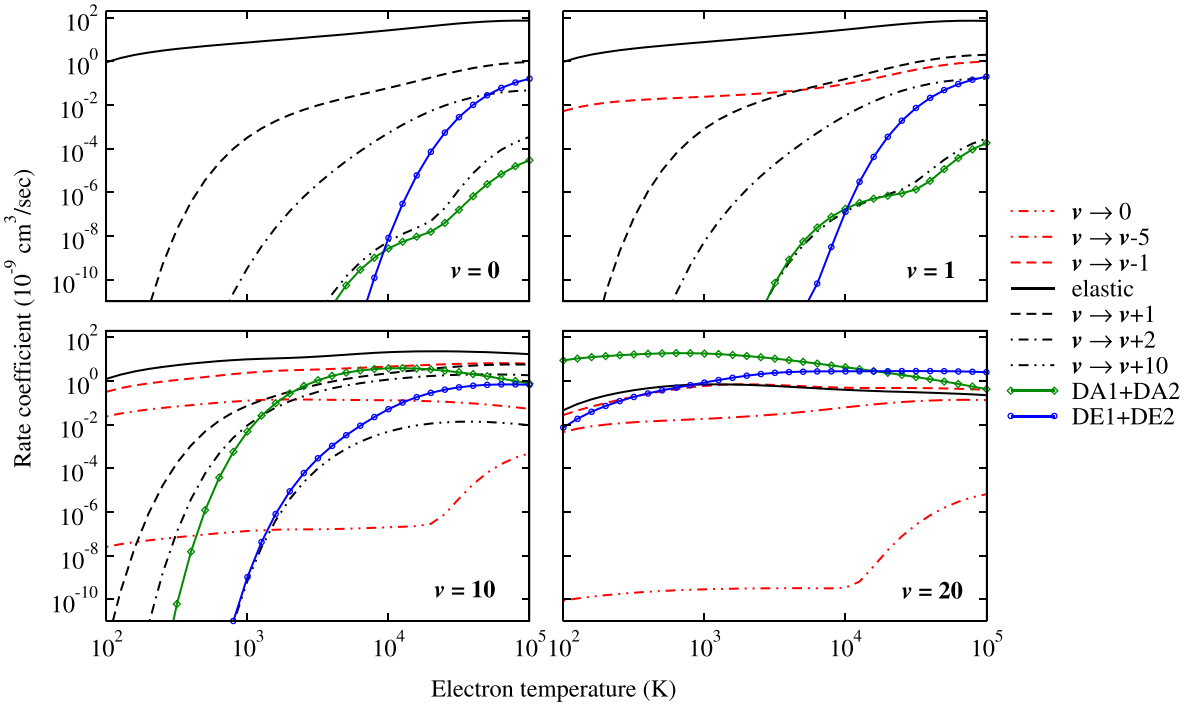

Figure 4. Selected vibrationally resolved Maxwellian rate coefficients for initial vibrational states $v = 0, 1, 10$ and 20, as a function of the electron temperature, for the ground state $X\,^1\Sigma_g^+$ of D_2 molecule and for the processes of vibrational excitation, dissociative attachment and dissociative excitation as obtained from the LCP model.

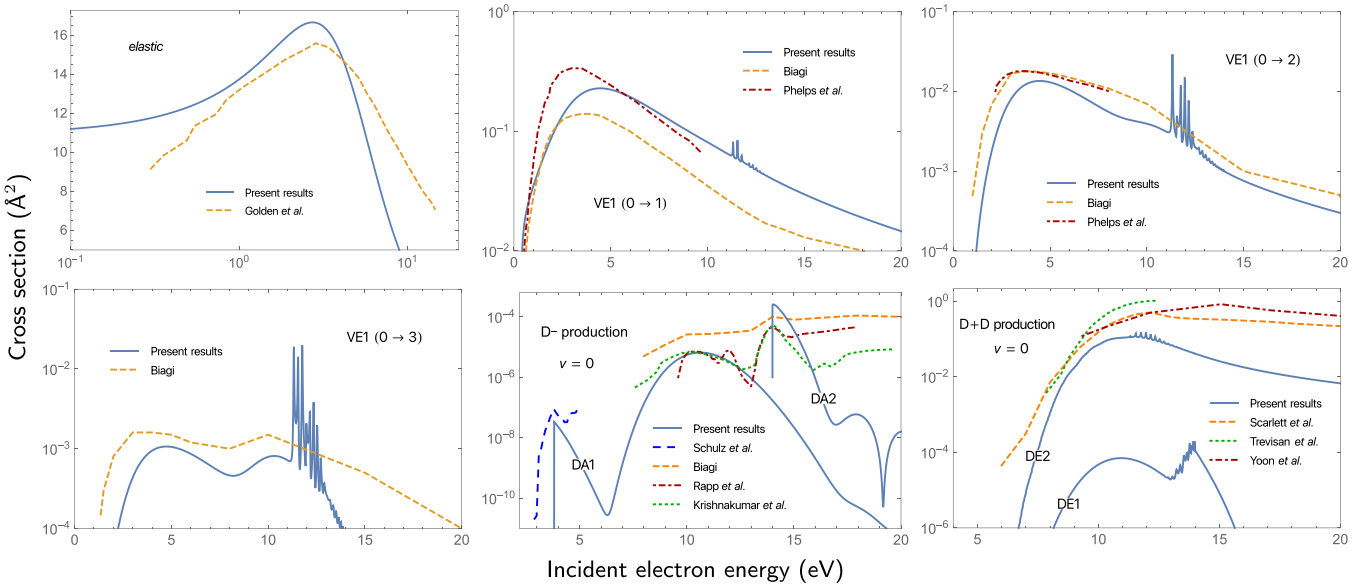

Figure 5. Comparison of cross sections obtained in the LCP approach with data present in the literature by Golden *et al* [52], Buckman and Phelps [54], Pitchford *et al* [55], Schulz and Asundi [56], Rapp *et al* [57], Krishnakumar *et al* [13], Scarlett *et al* [58], Trevisan and Tennyson [59] and Yoon *et al* [60] for the processes indicated in the plots.

numbers, the thresholds for DA and DE processes for H_2 decrease compared with those for D_2. Similarly, as a consequence of the fact that the spacing between vibrational levels is smaller for D_2 than for H_2, the threshold for the VE cross sections increases for H_2.

Concerning the magnitude and the shape of the cross sections, in general, H_2 has the same trend as D_2 but shifted towards higher energies. However, in some cases, see for example the 5→6 VE transitions, the structure of the resonant peaks is completely different.

We should point out, in particular, the factor of about 200 difference between H_2 and D_2, in the DA cross sections for $v = 0$, and for the 4 eV resonance. This is to be regarded as the major isotope effect for fusion plasmas: no DA process in deuterium plasmas are relevant at these collision energies, but in hydrogen plasmas still some noticeable H^- production

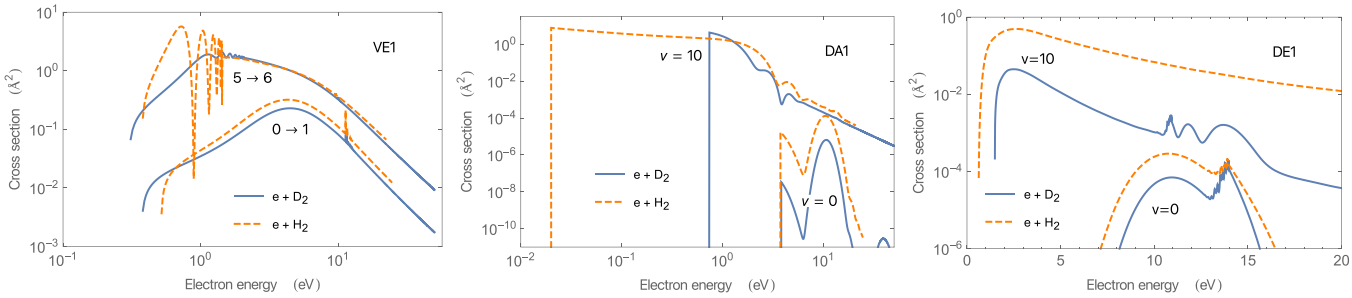

Figure 6. Isotopologue effect on cross sections of D_2 (solid line) and H_2 (dashed line) molecules for some processes of vibrational excitation, dissociative attachment and dissociative excitation.

(and subsequent mutual neutralization with protons) might be a relevant process channel. In fusion (divertor) plasmas one expects mostly $v = 0$ (or small amounts of $v = 1, 2$) vibrational states. Furthermore only the lowest 4 eV resonance (first peak in DA1 cross sections) should play a role, because molecules are rapidly destroyed. This strong suppression of the lowest DA1 channel in D_2 as compared to H_2 confirms, once again, the older findings, e.g. already of Rapp *et al* [57].

4. Conclusions

In conclusion, in this work, we presented a theoretical study on vibrationally-specific cross sections for electron deuterium resonant collisions within LCP formalism. We took into account three states of neutral deuterium molecule—including the ground $X\,^1\Sigma_g^+$, the dissociative $b\,^3\Sigma_u^+$ and the electronic $B\,^1\Sigma_u^+$ states—and three resonances of D_2^- anion. In our analysis, we considered the elementary processes listed in the table 1. In particular, for the first time, the LCP approach has been applied to study vibrational transitions and dissociation processes between different electronic states.

We observed the magnitude of the cross sections and the relative importance of the reactions varying over a large range of energy and in particular as a function of the initial electronic state and vibrational levels. This behavior relies basically on the specific coupling between the electronic states of the neutral D_2 and the anionic resonances.

Finally, we found good agreement with experimental data available in literature.

In the future works, we plan to extend the present calculations including excitation to other electronic excited states of D_2. In particular, for the couplings to the $^{1,3}\Pi$ states. Moreover, we intent to improve the model at low energies (temperatures) in order to determine rotational transitions.

Data availability statement

The data that support the findings of this study are openly available at the following URL/DOI: https://amdis.iaea.org/databases/ and LXCat database (www.lxcat.net/Laporta).

Acknowledgment

The authors thank Dr A Howling (Swiss Plasma Center, Lausanne, Switzerland) for careful reading of the manuscript and discussion. D R's work is carried out under the auspices of the ITER scientist fellowship program (ISFN).

ORCID iDs

V Laporta https://orcid.org/0000-0003-4251-407X
G Fubiani https://orcid.org/0000-0001-8920-9908
I Furno https://orcid.org/0000-0001-8348-1716
C Hill https://orcid.org/0000-0001-6604-0126
D Reiter https://orcid.org/0000-0001-5635-7103
F Taccogna https://orcid.org/0000-0001-9361-9010

References

[1] Krishnakumar E, Prabhudesai V S and Mason N J 2018 *Nat. Phys.* **14** 149
[2] Dalgarno A 2005 *J. Phys.: Conf. Ser.* **4** 002
[3] Galli D and Palla F 2013 *Annu. Rev. Astron. Astrophys.* **51** 163
[4] Lecluse C, Robert F, Gautier D and Guiraud M 1996 *Planet. Space Sci.* **44** 1579
[5] Kim Y H, Fox J L, Black J H and Moses J I 2014 *J. Geophys. Res.: Space Phys.* **119** 384
[6] Sang C, Stangeby P, Guo H and Wang D 2020 *Nucl. Fusion* **61** 016022
[7] Verhaegh K *et al* 2021 *Plasma Phys. Control. Fusion* **63** 035018
[8] Pitts R *et al* 2019 *Nucl. Mater. Energy* **20** 100696
[9] Sawada K and Goto M 2016 *Atoms* **4** 29
[10] Horáček J, Čížek M, Houfek K, Kolorenč P and Domcke W 2006 *Phys. Rev.* A **73** 022701
[11] Taccogna F and Minelli P 2017 *New J. Phys.* **19** 015012
[12] Bacal M and Wada M 2020 *Plasma Sources Sci. Technol.* **29** 033001
[13] Krishnakumar E, Denifl S, Čadež I, Markelj S and Mason N J 2011 *Phys. Rev. Lett.* **106** 243201
[14] Serianni G *et al* 2020 *Rev. Sci. Instrum.* **91** 023510
[15] Furno I, Agnello R, Fantz U, Howling A, Jacquier R, Marini C, Plyushchev G, Guittienne P and Simonin A 2017 *EPJ Web Conf.* **157** 03014
[16] Fubiani G *et al* 2021 in preparation
[17] Taccogna F, Minelli P, Bruno D, Longo S and Schneider R 2012 *Chem. Phys.* **398** 27
[18] Celiberto R *et al* 2017 *Atoms* **5** 18
[19] Wünderlich D and Fantz U 2016 *Atoms* **4** 26

[20] Meltzer T and Tennyson J 2020 *J. Phys. B: At. Mol. Opt. Phys.* **53** 245203
[21] Scarlett L H, Fursa D V, Zammit M C, Bray I, Ralchenko Y and Davie K D 2021 *At. Data Nucl. Data Tables* **137** 101361
[22] Zammit M C, Fursa D V and Bray I 2014 *Phys. Rev.* A **90** 022711
[23] Tapley J K, Scarlett L H, Savage J S, Zammit M C, Fursa D V and Bray I 2018 *J. Phys. B: At. Mol. Opt. Phys.* **51** 144007
[24] Allan M 1985 *J. Phys. B: At. Mol. Phys.* **18** L451
[25] van Wingerden B, de Heer F J, Weigold E and Nygaard K J 1977 *J. Phys. B: At. Mol. Phys.* **10** 1345
[26] Corrigan S J B 1965 *J. Chem. Phys.* **43** 4381
[27] Wrkich J, Mathews D, Kanik I, Trajmar S and Khakoo M A 2002 *J. Phys. B: At. Mol. Opt. Phys.* **35** 4695
[28] Tawara H, Itikawa Y, Nishimura H and Yoshino M 1990 *J. Phys. Chem. Ref. Data* **19** 617
[29] Zammit M C, Fursa D V and Bray I 2013 *Phys. Rev.* A **88** 062709
[30] Iacob F, Pop N, Mezei J Z, Epée M D E, Motapon O, Niyonzima S, Laporta V and Schneider I F 2019 *AIP Conf. Proc.* **2071** 020007
[31] Djuissi E *et al* 2020 *Rom. Astron. J.* **30** 101
[32] Chen F F 2016 *Kinetic Theory* (Cham: Springer International Publishing) pp 211–66
[33] Smirnov B M 2007 *Collisions Involving Electrons* (New York: Wiley) ch 4 pp 99–125
[34] Capitelli M, Ferreira C M, Gordiets B F and Osipov A I 2000 *Plasma Kinetics in Atmospheric Gases* (*Springer Series on Atomic, Optical and Plasma Physics*) (Berlin: Springer)
[35] Bardsley J N and Mandl F 1968 *Rep. Prog. Phys.* **31** 471
[36] Domcke W 1991 *Phys. Rep.* **208** 97
[37] Dubé L and Herzenberg A 1979 *Phys. Rev.* A **20** 194
[38] Houfek K, Rescigno T N and McCurdy C W 2006 *Phys. Rev.* A **73** 032721
[39] Laporta V, Schneider I F and Tennyson J 2020 *Plasma Sources Sci. Technol.* **29** 10LT01
[40] Laporta V, Tennyson J and Schneider I F 2020 *Plasma Sources Sci. Technol.* **29** 05LT02
[41] Laporta V, Cassidy C M, Tennyson J and Celiberto R 2012 *Plasma Sources Sci. Technol.* **21** 045005
[42] Laporta V, Celiberto R and Tennyson J 2013 *Plasma Sources Sci. Technol.* **22** 025001
[43] Laporta V, Celiberto R and Tennyson J 2015 *Phys. Rev.* A **91** 012701
[44] Laporta V, Heritier K and Panesi M 2016 *Chem. Phys.* **472** 44
[45] Kołos W and Wolniewicz L 1964 *J. Chem. Phys.* **41** 3663
[46] Sharp T 1970 *At. Data Nucl. Data Tables* **2** 119
[47] Kołos W and Wolniewicz L 1965 *J. Chem. Phys.* **43** 2429
[48] Wolniewicz L and Dressler K 1988 *J. Chem. Phys.* **88** 3861
[49] Bardsley J N and Wadehra J M 1979 *Phys. Rev.* A **20** 1398
[50] Celiberto R, Janev R K, Laporta V, Tennyson J and Wadehra J M 2013 *Phys. Rev.* A **88** 062701
[51] Stibbe D T and Tennyson J 1998 *J. Phys. B: At. Mol. Opt. Phys.* **31** 815
[52] Golden D E, Bandel H W and Salerno J A 1966 *Phys. Rev.* **146** 40
[53] Cooper G, Hitchcock A P and Chatzidimitriou-Dreismann C A 2008 *Phys. Rev. Lett.* **100** 043204
[54] Buckman S J and Phelps A V 1985 *J. Chem. Phys.* **82** 4999
[55] Pitchford L C *et al* 2017 *Plasma Process. Polym.* **14** 1600098
[56] Schulz G J and Asundi R K 1967 *Phys. Rev.* **158** 25
[57] Rapp D, Sharp T E and Briglia D D 1965 *Phys. Rev. Lett.* **14** 533
[58] Scarlett L H, Tapley J K, Fursa D V, Zammit M C, Savage J S and Bray I 2017 *Phys. Rev.* A **96** 062708
[59] Trevisan C S and Tennyson J 2002 *Plasma Phys. Control. Fusion* **44** 1263
[60] Yoon J-S, Kim Y-W, Kwon D-C, Song M-Y, Chang W-S, Kim C-G, Kumar V and Lee B 2010 *Rep. Prog. Phys.* **73** 116401